

《量子物理与材料化学杂志》

Journal of Quantum Physics and Materials Chemistry



ChengZhu Science™

江西省诚筑环保工程有限公司主办

2022 年 11 月刊物/Serial in November, 2022

出版人： 刘焕 香江出版社有限公司

Publisher: Liu Huan, Xiangjiang Publishing Company Ltd.



Copyrights Statements

Copying and Transferring is Forbidden!

版权申明

禁止复制、转载！

All the intellectual property (mainly including the original academic knowledges and brand logo) are prohibited to copy or transfer into other publications or websites. To cite this article, only short quote is acceptable, but copying or transferring any substantial part of this article is NOT allowed (Defined in <Copyright Ordinance> in Hong Kong). The original academic knowledge is the substantial part of an article as academic journal. For learning purpose, it is allowed to read our website in online video class only. This journal is published by Hong Kong Publisher, and the copyrights is regulated and protected by <Copyright Ordinance> in Hong Kong, China. This PDF document is accessible to public only through Hong Kong domain websites (natural-foundation-science.org), and its printed version is the formally published journal. Without permission, it is NOT allowed to print, issue and sale.

所有形式知识产权（主要包括原创型学术知识和品牌标识）禁止复制、转载到其他出版物和网站。如果需要引用这篇论文，仅仅允许简短引述，但是禁止复制、转载这篇论文中任何实质性部分（香港《版权条例》中定义）。作为学术杂志，这篇论文中的原创型学术知识即为作品的实质性部分。仅仅允许以学习为目的在线视频课堂阅读本公司网站。本杂志由香港出版社出版，其版权受中国香港《版权条例》监管和保护。此 PDF 文档仅仅通过香港主机网站向公众公开 (natural-foundation-science.org)，并且其印刷版本杂志为正式出版物。未经许可，不得印刷、发行、销售。

Article 10. Ancient Chinese Eight Diagrams and Application on Chemistry Reaction Rate/八卦与矩阵运算及其在化学反应速率中的应用研究

Author: Liu Huan (1983-), Master of Science (First Class Honours, 2009), The University of Auckland.

DOI: [10.58473/JQPMC0010](https://doi.org/10.58473/JQPMC0010) Retrieval from official database: www.crossref.org

Latest revised on 14/09/2024.

Ancient Chinese Eight Diagrams is created by the first King in Chinese race by literature, Fuxi. This is a tool to deduce and analyze the inter-relationships across materials or affairs consisting of five elements (Metal, Wood, Water, Fire and Soil) at both temporal and spacial scales, with the key philosophy of Yin and Yang (translation as negative and positive poles respectively). As discussed in this journal, the basic attribute of materials contains magnetism, so the first one presenting this philosophy is just Fuxi in literature. The method of deducing and analyzing the inter-relationships across materials or affairs by Ancient Chinese Eight Diagrams is the embryo of matrix and linear algebra. However, for the matrix designed in this article, 0 represents negative pole and 1 represents positive pole like the matrix designed for genetic algorithm in this journal, and the philosophy of this originates from the Ancient Chinese Eight Diagrams. This binary algebra usually is applicable on the micro-scale substances. However, for the classification of bio-communities in a ecosystem, which possesses more advanced intelligence, more complex matrix is required. Unlike Taoists who utilize this tool to predict people's fate or fortune, this book aims to succeed the philosophy of Ancient Chinese Eight Diagrams and further develop this on bio-medicine engineering or chemical engineering. This article aims to build a 3D model for the estimation of chemistry reaction rate at both spacial and temporal scales.

Hypotheses: in the spacial grid unit designed in this 3D modeling, the molecule motion frequently and regularly passes through this spacial grid unit. If this molecule motion exactly passes through this spacial grid unit, the magnetism value in this point is defined as 1; if this molecule motion leaves this spacial grid unit, the magnetism value in this point is defined as 0. Then the matrix of this spacial grid unit is defined as:

Matrix A = [a1,a2,a3,...]

Matrix B = [b1,b2,b3,...]

In this matrix, a1 is the magnetism value at time T1; a2 is the magnetism value at time T2; a3 is the magnetism value at time T3..... ;And a1, a2, a3 ... are the value 0 or 1. Matrix B is the same definition.

Spatial and Temporal Scales: the size of spacial grid unit designed in this 3D modeling is determined by the Max molecular length, and the parameter of time interval between T1 and T2 is determined by the molecular motion speed which required experiment test for parameterization. The Max molecular length is not necessary to be the very exact one, because usually when two molecules approach each other (does not need to exactly collide each other) at specific intersection angel, chemistry reaction occurs. Hence the size of spacial grid unit can be easily estimated according to the published molecular length of relevant chemistry species.

Matrix A is the matrix representing molecule A; Matrix B is the matrix representing molecule B. Chemistry reaction occurs between molecule A and molecule B. Only once molecule A and molecule B collides at specific intersection angle (or angles) of spacial magnetism curves between two molecule A and B, chemistry reaction occurs. The other intersection angles between molecule A and B collision can not lead to chemistry reaction. Consequently, it is hypothesized that molecule motion shows equal or random chances of occurrence in each spacial grid unit along motion orbit, which can be derived by the molar volume or molar concentration of chemistry molecules. With the chemistry reaction process, the chances of occurrence in each spacial grid unit decreases with the reduction in molar concentrations of molecule A and B, which can be edited into this 3D modeling as sub-models.

Then the occurrence of collision between molecule A and B in a spacial grid unit is calculated as:

$$\text{Chemistry Reaction Rate} = P_a \times \text{Matrix A} \times P_b \times (\text{Matrix B})^T = P_a \times P_b \times [a_1*b_1, a_2*b_2, a_3*b_3, \dots], (\text{Matrix B})^T \text{ is the transpose of Matrix B}$$

In this matrix, if $a_1*b_1 = 0$, there is no occurrence of collision between two molecule A and B in a spacial grid unit; if $a_1*b_1 = 1$, collision between two molecules occurs in a spacial grid unit...; However, only once molecule A and molecule B collides at specific intersection angle (or angles) of spacial magnetism curves between two molecule A and B, chemistry reaction occurs. Consequently, P_a and P_b is the proportion of the specific spherical surface area of active chemistry bonds in molecule A and molecule B respectively, to its whole spherical surface area of a molecule during the molecular revolution, depended on the molecular structure. This can be derived from the 3D graph design of chemistry molecule.

Then the spacial diffusion models, such us Gaussian diffusion model, can be easily incorporated into this 3D modeling as sub-models, which determines the initial concentrations of each chemistry species in spatial distribution. These spatial distribution models (such us Gaussian diffusion model) usually focus on the chemistry transport only and do not consider the chemistry reaction conversions between chemistry species, so my model should fill in the academic/technological blanks. This matrix reflects the inter-dependent effects between two symmetric time

spaces along the fourth dimension axis [1]. Please note: the sequence of steps in building up this model is also significantly different from the models set up in our Environmental Modeling Lab, so coping and transferring this sequence of steps is not allowed, which should be original too.

Once the modeling chemistry reaction rate is compared and contrasted with the experimental test rate of chemistry reaction, it is easily to deduce the molecule motion speed under experimental conditions by this 3D modeling as parameterization. Consequently, the spacial points of intersection among the motion orbits of different molecules can be deduced by test and 3D graph. Obviously, the orbits of molecule motion is sphere shape, forming electromagnetic waves diffused around this.

To more accurately simulate the chemistry reaction rate, the frequency of molecule spinning motion is introduced into this 3D modeling, so the equation can be improved into:

$$\text{Chemistry Reaction Rate} = P_a \times \text{Matrix A} \times P_b \times (\text{Matrix B})^T \times F_a \times F_b$$

F_a and F_b represents the frequency of molecule spinning motion in molecule A and B respectively, which can be estimated according to the electromagnetic wave detector. Electromagnetic wave detector measures the electromagnetic waves generated by molecule spinning motion. The theory of this estimation has been further discussed in this article[4][7].

This 3D modeling does not only provide the empirical methods to calculate the results of chemistry reaction like this numerical modeling [3], but also plays the role in theoretical model to help to better understand the mechanism of chemistry reactions: Firstly, increased thermal energy increases the frequency of molecule motion along orbit and alters the structure of spacial magnetism curves in a molecule, which triggers the threshold energy for chemistry reaction. The effects of particles' thermal motion on the electron magnetic moment is discussed in this paper [2], which means that the spherical surface area of active chemistry bonds in this 3D modeling increases under external thermal effects, to reach the threshold thermal energy for chemistry reaction (such as ignition point). It is easy to understand that the irregular thermal motion of free electrons is strengthened under externally increased temperature, so the spherical surface area of active chemistry bonds tends to increase correspondingly in this 3D modeling; Secondly, the effects of catalyzer can be also modeled by increasing the spherical surface area of active chemistry bonds in molecule revolution motion when catalyzer agents are applied. If the catalyzer agents are added to bind molecule A firstly, the spherical surface area of active chemistry bonds must be bigger in the molecules of catalyzer agents in comparison to the molecule B, accelerating synthesis velocity, while the spherical surface area of active chemistry bonds must be bigger in the molecules of intermediate products compared with molecule A, facilitating the synthesis between intermediate products and molecule B,

which yields the final products and catalyzer agents. Because the catalyzer agents remain unchanged after this chemistry reaction process, it is easy to understand that the effects of catalyzer can be directly expressed by increasing the spherical surface area of active chemistry bonds during molecule A revolution motion in this 3D modeling; Thirdly, once the motion rhythm of spacial magnetism curves in synthesized molecule leads to higher thermal energy than previous molecules, which can be modeled by higher frequency of molecule spinning motion in synthesized molecule, this is the exothermic reaction; once the motion rhythm of spacial magnetism curves in synthesized molecule leads to lower thermal energy than previous molecules, which can be modeled by lower frequency of molecule spinning motion in synthesized molecule, this is the endothermic chemistry reaction.

The modeling of thermal effects measured by temperature, which is divided into thermal energy generated by molecule spinning motion (expressed as the function of the frequency of molecule spinning motion) and thermal energy produced by molecule motions across different spacial grids (expressed as the function of the motion speed across different spacial grids). The theory of this has been discussed in this article [5]. The parameters of these two parts can be measured by electromagnetic wave detector and experimental test rate of chemistry reaction as discussed above.

Modeling of the formation of magnetic materials by binary arithmetic: the formation mechanism of magnetic materials is discussed in my previous article [2], which can be simulated by another 3D modeling. In a new model, each molecule is evenly divided into 8 spacial grids. If the electron clouds or orbits in a spacial grid is clockwise orientation, its value is set to be 0 as Yin pole; If the electron clouds or orbits in a spacial grid is anti-clockwise orientation, its value is set to be 1 as Yang pole; Modeling of symmetric magnetism: if there is collision between two molecules, and the adjacent spacial grids between these two molecules is symmetric magnetism, which means that one is clockwise orientation as 0 value and the other is anti-clockwise orientation as 1 value, it strengthens the formation of magnetic materials. If the adjacent spacial grids between these two molecules is asymmetric magnetism, which means that two spacial grids show the same orientation orbits, they generate repulsive force against each other; the motion orbit of the central points of a molecule is set as random probability in each spacial grid, driven by thermal energy effects. Obviously, if there is more symmetric spacial array as [0,1] or [1,0] value by binary arithmetic, this materials tends to be ferromagnetism; if there is more asymmetric spacial array, including [0,0] and [1,1] by binary arithmetic, this materials tends to be anti-ferromagnetism. The probability of both symmetric spacial array and asymmetric spacial array in each grid can be simulated and estimated by this theoretical 3D modeling.

Modeling of electron cloud: in a new sub-model, each atom is evenly divided into 64 spacial grids. Then it is to model the spinning of electron cloud as: if the electron clouds or orbits in a spacial grid is clockwise orientation, its value is set to be - 1 as

Yin pole; if the electron clouds or orbits in a spacial grid is anti-clockwise orientation, its value is set to be +1 as Yang pole. It is further to model the density of electron cloud, which is measured by magnetic flux: if the density of electron cloud in a spacial grid is higher, then the probability of electron occurrence \times electron quantity in this spacial grid is higher, so that the magnetic flux within unit temporal scale in this spacial grid is stronger. The overall magnetic flux of an atom is the vector sum of magnetic flux in each spacial grid. For the highly symmetric electron clouds of an atom, the overall magnetic flux tends to be zero, revealing high stability in chemistry activity. In comparison, the asymmetric magnetic flux in spatial grids represents the free electron orbits. Then the more spatial grids of asymmetric magnetic flux, or the more asymmetric overall magnetic flux of an atom, the broader spherical surface area of active chemistry bonds in atom spinning motion, the more active in chemistry reaction. My another article has demonstrated that the quantity of electric charges must be different between clockwise spinning electrons and anticlockwise spinning electrons in electron clouds [6]. Therefore, constant j and k are given to the clockwise spinning electrons and anticlockwise spinning electrons in electron clouds respectively, when the quantity of electric charges is modeled to represent the difference in electric charges between two types. For the electrons with higher electric charges, the total electron energy is higher, the chemistry bond energy required to activate the reaction is lower, so the chemistry reaction is more active correspondingly. When the parameter of chemistry bond energy is added in this 3D modeling, the chemistry reaction rate is calculated as:

$$\text{Chemistry Reaction Rate} = P_a \times \text{Matrix A} \times P_b \times (\text{Matrix B})^T \times F_a \times F_b \times 1/E_a \times 1/E_b$$

Where E_a , E_b represents the chemistry bond energy for active chemistry bond A and B respectively. According to the definition of chemistry bond energy in quantum chemistry, the E_a , E_b is the function of the overall magnetic flux of an atom, which will be further discussed and quantified in the coming article [7].

In this paper, the Chinese Eight Diagrams matrix operation essentially reflects that the magnetic line in the fourth dimension coordinate between two symmetric three-dimensional spaces dominates the motion law of microscopic particles. Its theory has been fully discussed in previous papers [1][2]. In this paper, the 3D modeling sets the occurrence probability of the particle motion trajectory in each spatial grid cell as the random one, but the probability distribution of randomness is still subject to statistical laws (such as normal distribution rate), which is fundamentally different from the disorder of probability. Just because the distribution probability of microscopic particles on the spatial motion trajectory is subject to the statistical laws, it can be predicted and modeled by the simulation. If it is the disordered motion trajectory, it cannot be estimated by the modeling. Thus, it also reveals that the magnetic line between two symmetric three-dimensional spaces is an intelligent magnetic line dominated by biotic forces.

译文：本文八卦矩阵运算从本质上反映了第四维度坐标上两个对称三维物质空间之间的磁力线主导着微观粒子的运动规律。其理论在之前论文已经充分论述 [1][2]。本文空间模拟把粒子运动轨迹在各个空间网格单元中的出现概率设置为随机型，但是随机性的概率分布仍然在统计学上服从统计规律（比如正态分布率），与概率分布的无序性有本质区别。正是因为微观粒子在空间运动轨迹上的分布概率服从统计学规律，才能被模拟预测出来。如果是无序性的运动轨迹，则不可被模拟预测。从而也说明，两个对称三维物质空间之间的磁力线是一种有生力量在主导的智慧型磁力线。

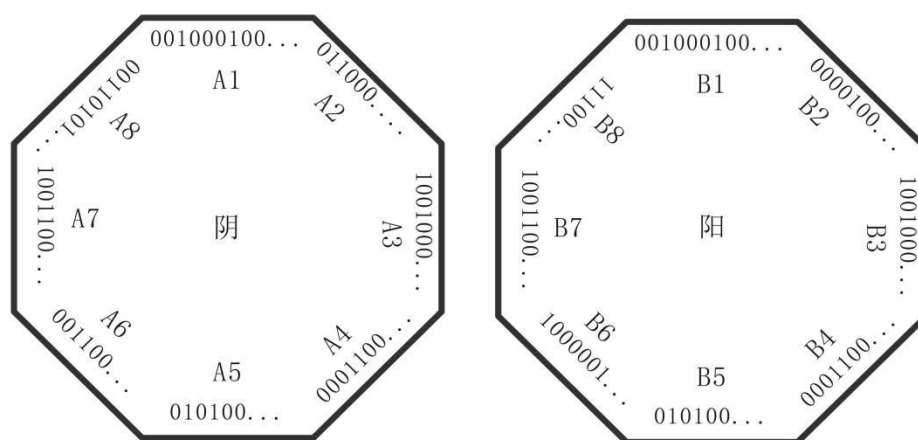


图 1. 八卦阵阴、阳二阵的排列组合。

八卦阵的神奇算术：

以上两个图片分别为阴、阳二阵，阴阵为矩阵 $A=[A1, A2, \dots, A8]$ ，阳阵为矩阵 $B=[B1, B2, \dots, B8]$ ，其中 A1 与 B1 为 0, 1 二位进制算法的随机型数字（如图 所示）排列组合，并且分别为矩阵 A 和 B 的第一列。与 A1 和 B1 相似，矩阵 A 和 B 中其它列中的数值亦为 0, 1 二位进制算法的随机型数字排列组合。阴阳二阵的相互作用关系表达为矩阵 A 乘以矩阵 B 的倒置。每隔一段时间 T，矩阵就像时钟一样旋转一格，旋转一圈是一共八格。如图例所示，阴阵顺时针方向旋转一格，矩阵 A 则变化为 $[A8, A1, A2, \dots, A7]$ ，阴阳二阵的相互作用关系表达为变化后的矩阵 A 乘以矩阵 B 的倒置。之后再次旋 转一格，矩阵变化则以此类推。

神奇算术：每旋转一圈，A 和 B 中的 0, 1 二位进制算法的数字排列组合就会重新随机型选取一次，代表阴、阳二阵中的事物随着时间发生变动，但是最终的

行列式运算结果总体上一定符合统计学规律，并非无序性。如果喜欢应用数学，可以通过模拟计算并且探讨。

八卦矩阵算术反映了宇宙阴、阳两极的相互作用关系，本文已经应用于模拟微观粒子的运动轨迹，其中二进制算法用于表示第四维度坐标上的磁力线在空间单元网格中是否出现。这类二进制算法不仅可以普遍应用于电路设计、天体物理学、生态环境评价等自然科学领域，也可以应用于“是、否”“有、无”等逻辑关系的社会科学领域。以下程序为应用 C++ 语言编写阴阳二矩阵的顺时针转动变化与乘积：

```
#include <bits/stdc++.h>
using namespace std;
int a[101][101],b[101][101],c[101][101],d[101][101],e[101][101],f[101][101],
g[101][101],h[101][101],i[101][101],j[101][101],k[101][101],l[101][101],m[101][
101],n[101][101],o[101][101],p[101][101],q[101][101],r[101][101];
int main ()
{
    int i,j,n,t;
    cin>>n;
    for(i=1;i<=n;i++)
        for(j=1;j<=8;j++)
            cin>>a[i][j]; //输入阴阵的赋值， a[i][j]可以为 0 或者 1

    for(i=1;i<=n;i++)
        for(j=1;j<=8;j++)
            cin>>b[i][j]; //输入阳阵的赋值， b[i][j]可以为 0 或者 1

    cout<<endl;

    for(i=1;i<=8;i++)
        for(j=1;j<=n;j++)
            c[i][j]=b[j][i]; //导出阳阵的倒置

    for(i=1;i<=n;i++)
        for(j=1;j<=n;j++)
            for(t=1;t<=8;t++)
            {
                d[i][j]+=a[i][t]*c[t][j]; //算出阴阵与阳阵倒置相乘的值
            }

    for(i=1;i<=n;i++)
    {
        for(j=1;j<=n;j++)
            cout<<d[i][j]<<" "; //输出阴阵与阳阵倒置乘积矩阵 (n*n)
    }
}
```

```

        cout<<endl;
    }
    cout<<endl;

for(i=1;i<=n;i++)
{
    for(j=1;j<=8;j++)
    {
        if(j==1) e[i][j]=a[i][8];
        else e[i][j]=a[i][j-1];    //阴阵顺时针转动一格之后的矩阵变形
    }
}

for(i=1;i<=n;i++)
    for(j=1;j<=n;j++)
        for(t=1;t<=8;t++)
            f[i][j]+=e[i][t]*c[t][j];    //算出阴阵变换之后与阳阵倒置相乘的值

for(i=1;i<=n;i++)
{
    for(j=1;j<=n;j++)
        cout<<f[i][j]<<" ";    //输出阴阵与阳阵倒置乘积矩阵 (n*n)
    cout<<endl;
}
cout<<endl;

for(i=1;i<=n;i++)
{
    for(j=1;j<=8;j++)
    {
        if(j==1) g[i][j]=e[i][8];
        else g[i][j]=e[i][j-1];    //阴阵再次顺时针转动一格之后的矩阵变形
    }
}

for(i=1;i<=n;i++)
    for(j=1;j<=n;j++)
        for(t=1;t<=8;t++)
            H[i][j]+=g[i][t]*c[t][j];    //算出阴阵变换之后与阳阵倒置相乘的值

for(i=1;i<=n;i++)
{
    for(j=1;j<=n;j++)
        cout<<H[i][j]<<" ";    //输出阴阵与阳阵倒置乘积矩阵 (n*n)
}

```

```

    cout<<endl;
}
cout<<endl;

for(i=1;i<=n;i++)
{
    for(j=1;j<=8;j++)
    {
        if(j==1) I[i][j]=g[i][8];
        else I[i][j]=g[i][j-1]; //阴阵再次顺时针转动一格之后的矩阵变形
    }
}

for(i=1;i<=n;i++)
    for(j=1;j<=n;j++)
        for(t=1;t<=8;t++)
            J[i][j]+=I[i][t]*c[t][j]; //算出阴阵变换之后与阳阵倒置相乘的值

for(i=1;i<=n;i++)
{
    for(j=1;j<=n;j++)
        cout<<J[i][j]<<" "; //输出阴阵与阳阵倒置乘积矩阵 (n*n)
    cout<<endl;
}
cout<<endl;

for(i=1;i<=n;i++)
{
    for(j=1;j<=8;j++)
    {
        if(j==1) K[i][j]=I[i][8];
        else K[i][j]=I[i][j-1]; //阴阵再次顺时针转动一格之后的矩阵变形
    }
}

for(i=1;i<=n;i++)
    for(j=1;j<=n;j++)
        for(t=1;t<=8;t++)
            L[i][j]+=K[i][t]*c[t][j]; //算出阴阵变换之后与阳阵倒置相乘的值

for(i=1;i<=n;i++)
{
    for(j=1;j<=n;j++)
        cout<<L[i][j]<<" "; //输出阴阵与阳阵倒置乘积矩阵 (n*n)
}

```

```

        cout<<endl;
    }
    cout<<endl;

    for(i=1;i<=n;i++)
    {
        for(j=1;j<=8;j++)
        {
            if(j==1) M[i][j]=K[i][8];
            else M[i][j]=K[i][j-1]; //阴阵再次顺时针转动一格之后的矩阵变形
        }
    }

    for(i=1;i<=n;i++)
        for(j=1;j<=n;j++)
            for(t=1;t<=8;t++)
                N[i][j]+=M[i][t]*c[t][j]; //算出阴阵变换之后与阳阵倒置相乘的值

    for(i=1;i<=n;i++)
    {
        for(j=1;j<=n;j++)
            cout<<N[i][j]<<" "; //输出阴阵与阳阵倒置乘积矩阵 (n*n)
        cout<<endl;
    }
    cout<<endl;

    for(i=1;i<=n;i++)
    {
        for(j=1;j<=8;j++)
        {
            if(j==1) O[i][j]=M[i][8];
            else O[i][j]=M[i][j-1]; //阴阵再次顺时针转动一格之后的矩阵变形
        }
    }

    for(i=1;i<=n;i++)
        for(j=1;j<=n;j++)
            for(t=1;t<=8;t++)
                P[i][j]+=O[i][t]*c[t][j]; //算出阴阵变换之后与阳阵倒置相乘的值

    for(i=1;i<=n;i++)
    {
        for(j=1;j<=n;j++)
            cout<<P[i][j]<<" "; //输出阴阵与阳阵倒置乘积矩阵 (n*n)
    }

```

```

    cout<<endl;
}
cout<<endl;

for(i=1;i<=n;i++)
{
    for(j=1;j<=8;j++)
    {
        if(j==1) Q[i][j]=O[i][8];
        else Q[i][j]=O[i][j-1]; //阴阵再次顺时针转动一格之后的矩阵变形
    }
}

for(i=1;i<=n;i++)
    for(j=1;j<=n;j++)
        for(t=1;t<=8;t++)
            R[i][j]+=Q[i][t]*c[t][j]; //算出阴阵变换之后与阳阵倒置相乘的值

for(i=1;i<=n;i++)
{
    for(j=1;j<=n;j++)
        cout<<R[i][j]<<" "; //输出阴阵与阳阵倒置乘积矩阵 (n*n)
    cout<<endl;
} //一共输出 8 个 (n*n) 矩阵用以统计运算

    return 0;
}

```

Please note: This is the revised materials in book “Proceedings for Degree of Postgraduate Diploma in Environmental Science (3rd Edition).” published in 2016. Firstly revised on 31/ 12/2020; Secondly revised on 20/ 11/2021; Thirdly revised on 21/ 11/2021; Fourthly revised on 30/01/2022; Fifthly revised on 17/02/2022. This journal article is previously published as: Liu Huan. (2021). Ancient Chinese Eight Diagrams and Application on Chemistry Reaction Rate. Journal of Environment and Health Science (ISSN 2314- 1628), 2021(02)., which is converted into Journal of Quantum Physics and Materials Chemistry (ISSN2958-4027) . Both Journals belong to the same publisher, Liu Huan. The previous journal article is closed to the public, but the previous reference is still valid. Latest revised on 04/02/2023; 05/02/2023; 06/02/2023;08/02/2023a; 08/02/2023b; 08/02/2023c; 10/02/2023; 12/02/2023; 22/05/2023;26/05/2023;07/06/2023; 12/06/2023; 03/08/2023 **a;b**; 04/08/2023; 05/08/2023; 08/11/2023 **a;b**;21/11/2023;09/09/2024;10/09/2024; 11/09/2024;14/09/2024.

Copyrights Notice: due to the absence of commercial license to Netlogo software, the application plans of 3D modeling based on Netlogo is abandoned; We have never started to built this 3D modeling by using Netlogo software before and have never published or distributed any programs edited by using Netlogo before; The C++ program has been used instead of Netlogo software. Please note that the GNU General Public License is not applicable on any materials published in this article, and all the copyrights of this article is exclusively owned and protected by <Copyrights Ordinance> in Hong Kong.

References:

- [1]. Liu Huan. (2021). The anti-matter of symmetric three-dimensional spaces along the fourth dimension axis. Journal of Environment and Health Science (ISSN 2314- 1628), 2021(2). <https://doi.org/10.58473/JAES0002>
- [2]. Liu Huan. (2022). Essay: Electromagnetics and Materials. Journal of Environment and Health Science (ISSN 2314- 1628), 2022(11). <https://doi.org/10.58473/JQPMC0004>
- [3]. Liu Huan (2021). Modeling of annual net primary production of a forest in the Taramakau Valley, Westland, New Zealand. Journal of Environment and Health Science (ISSN 2314- 1628). 2021(2). <https://doi.org/10.58473/JEHS0007>
- [4]. Liu Huan (2021). The particle dualism of electromagnetic waves. Journal of Environment and Health Science (ISSN 2314- 1628), 2021(2). <https://doi.org/10.58473/JQPMC0002>
- [5]. Liu Huan. (2021). The Principal of Thermodynamics: The Inner Energy, Energy Loss and Materials Perishing. Journal of Environment and Health Science (ISSN 2314- 1628), 2021(02). <https://doi.org/10.58473/JQPMC0008>
- [6]. Liu Huan (2023). Essay: original review of high-dimensional spaces and astronomy theories in modern physics. Journal of Astronomy and Earth Sciences (ISSN2958-4043). 2023 (07). <https://doi.org/10.58473/JAES0010>
- [7]. Liu Huan. (2023). Original review of quantum chemistry and 3D modeling of artificial intelligence. Journal of Quantum Physics and Materials Chemistry (ISSN2958-4027). 2023(11). <https://doi.org/10.58473/JQPMC0013>